HHS Public Access

Author manuscript

Neuroscience. Author manuscript; available in PMC 2019 July 15.

Published in final edited form as:

Neuroscience. 2018 July 15; 383: 60–73. doi:10.1016/j.neuroscience.2018.05.003.

LONG-TERM REDUCTIONS IN THE POPULATION OF GABAERGIC INTERNEURONS IN THE MOUSE HIPPOCAMPUS FOLLOWING DEVELOPMENTAL ETHANOL EXPOSURE

Clark W. Bird[a], **Devin H. Taylor**[a,1], **Natalie J. Pinkowski**[a,2], **G. Jill Chavez**[a], and **C. Fernando Valenzuela**[a]

[a]Department of Neurosciences, School of Medicine, University of New Mexico Health Sciences Center, Albuquerque, New Mexico, U.S.A

Abstract

Developmental exposure to ethanol leads to a constellation of cognitive and behavioral abnormalities known as Fetal Alcohol Spectrum Disorders (FASDs). Many cell types throughout the central nervous system are negatively impacted by gestational alcohol exposure, including inhibitory, GABAergic interneurons. Little evidence exists, however, describing the long-term impact of fetal alcohol exposure on survival of interneurons within the hippocampal formation, which is critical for learning and memory processes that are impaired in individuals with FASDs. Mice expressing Venus yellow fluorescent protein in inhibitory interneurons were exposed to vaporized ethanol during the third trimester equivalent of human gestation (postnatal days 2-9), and the long-term effects on interneuron numbers were measured using unbiased stereology at P90. In adulthood, interneuron populations were reduced in every hippocampal region examined. Moreover, we found that a single exposure to ethanol at P7 caused robust activation of apoptotic neurodegeneration of interneurons in the hilus, granule cell layer, CA1 and CA3 regions of the hippocampus. These studies demonstrate that developmental ethanol exposure has a long-term impact on hippocampal interneuron survivability, and may provide a mechanism partially explaining deficits in hippocampal function and hippocampal dependent behaviors in those afflicted with FASDs.

Corresponding Author: C. Fernando Valenzuela, M.D., Ph.D., Department of Neurosciences, MSC08 4740, 1 University of New Mexico, Albuquerque, NM 87131-0001, Phone: (505) 272-3128, Fax: (505) 272-8082, fvalenzuela@salud.unm.edu.

[1]Present address: Department of Biology, Utah Valley University, Orem, Utah, U.S.A.

[2]Present address: Department of Psychology, San Diego State University, San Diego, California, U.S.A.

Declarations of interest: none.

Author contributions: CWB, DHT, CFV designed experiments; CWB, DHT, NJP, and GJC performed experiments; CWB, DHT, NJP, CFV analyzed data; CWB and CFV interpreted results; CWB wrote the manuscript; CFV and DHT edited the manuscript.

WEB REFERENCES

Allen Brain Institute's nissl-stained sagittal atlas of the developing P7 mouse brain. Last accessed 4/9/2017. http://developingmouse.brain-map.org/experiment/siv?id=100073790&imageId=101229765&initImage=nissl

Keywords

Interneuron; hippocampus; apoptosis; fetal; alcohol; ethanol; development

INTRODUCTION

Gestational exposure to ethanol (EtOH) is one of the leading preventable causes of cognitive, physiological, and behavioral deficiencies in children around the world (Autti-Rämö and Granström, 1991; Hamilton et al., 2003; Kodituwakku, 2007; Mattson and Riley, 1999; Mattson et al., 2013; Riley et al., 2011; Simmons et al., 2010). Collectively, deficits induced by EtOH exposure during development are categorized under the umbrella diagnosis of Fetal Alcohol Spectrum Disorders (FASDs), which includes Fetal Alcohol Syndrome, partial FAS, and alcohol-related neurodevelopmental disorders (Chasnoff et al., 2010; May et al., 2014). Despite educational outreach efforts to inform the public on the dangers of exposing the developing fetus to EtOH, a relatively high percentage (2-5%) of children in the United States are exposed to some amount of alcohol during gestation (May et al., 2014), and in some populations up to 63% of children are exposed to EtOH in the womb (Miguez et al., 2009). Children afflicted with FASDs present with an assortment of problems in learning and memory processes, which result, at least in part, from dysfunction within the hippocampal region of the brain (Berman and Hannigan, 2000; Hamilton et al., 2003; Mattson et al., 1996; Uecker and Nadel, 1996, 1998). The hippocampus receives input via the perforant path from superficial layers of the entorhinal cortex, which synapse onto dendrites from granule cells of the dentate gyrus. Granule cells then project mossy fibers to CA3 pyramidal cells, which in turn synapse onto CA1 pyramidal neurons via Schaffer collaterals (Ribak and Shapiro, 2007). This well-characterized tri-synaptic circuit is intricately regulated by inhibitory, gamma-aminobutyric acid (GABA) expressing interneurons (Kullmann, 2011). Interneurons represent a minority of neurons in the hippocampus (10-20%) (Freedman et al., 1993; Olbrich and Braak, 1985), but because of their dense axonal arborization, they can innervate hundreds of postsynaptic target dendrites (Lubke et al., 1998; Muller and Remy, 2014; Savanthrapadian et al., 2014), providing tight regulation of circuit level signaling within the hippocampus (Cobb et al., 1995).

GABAergic interneurons are particularly vulnerable to a variety of insults, including excitotoxicity (Shetty et al., 2009; Shetty and Turner, 2001), ischemic events (Bering et al., 1997; Johansen, 1993), and traumatic brain injury (Lowenstein et al., 1992; Schiavone et al., 2017). Previous research has also demonstrated that interneurons in a variety of brain regions are susceptible to damage by both developmental and postnatal EtOH exposure (Andrade et al., 1992; Moore et al., 1998). Developmental exposure to EtOH reduces interneuron populations in cortical areas (Miller, 2006; Moore et al., 1998; Smiley et al., 2015), and in the cerebellum (Nirgudkar et al., 2016). Relatively little information exists, however, on the impact of developmental EtOH exposure on hippocampal interneuron populations. (Miki et al., 2000) demonstrated that exposure to EtOH during the third trimester equivalent of human gestation in the rat reduced the number of neurons in the hilus of the dentate gyrus, which is an area that contains an abundance of interneurons, but did not specifically identify interneurons in their study. Another set of experiments demonstrated

that a single postnatal EtOH exposure led to long-term reductions in parvalbumin (PV)-expressing interneurons in the CA1 region of the mouse brain (Sadrian et al., 2014).

Developmental EtOH exposure causes robust activation of programmed cell death via apoptotic signaling pathways in a variety of cells throughout the brain (Ikonomidou et al., 2000; Olney et al., 2002), including the hippocampus (Camargo Moreno et al., 2017). Until recently, it has remained unknown whether reductions in interneurons caused by developmental EtOH exposure are a result of apoptosis. A recent short report demonstrated that a single dose of EtOH during the early postnatal period increases the expression of cleaved caspase-3, a marker of apoptosis, in interneurons of the hippocampus (Ogievetsky et al., 2017). In the present study, we sought to further understand the effects of early postnatal EtOH exposure on hippocampal interneurons. Using a transgenic mouse model that expresses Venus fluorescent protein in GABAergic interneurons throughout the brain (Wang et al., 2009), mice were exposed to EtOH during the third trimester equivalent of human gestation, which mimics an exposure pattern observed in humans (Ethen et al., 2009). This period of development is also critical for refinement of neuronal circuits impacted by GABAergic signaling (Cellot and Cherubini, 2013; Le Magueresse and Monyer, 2013). We measured the density of interneurons expressing a marker of activated apoptosis in different hippocampal regions, and assessed the number of surviving interneurons in aged mice to understand the long-term trajectory of interneuron numbers in the hippocampus following developmental EtOH exposure.

EXPERIMENTAL PROCEDURES

All experimental procedures described adhered to the U.S. Public Health Service policy on humane care and use of laboratory animals and were approved by the Institutional Care and Use committee of the University of New Mexico Health Sciences Center. For all the experiments described below, experimenters were blinded to treatment group assignment.

Subjects

Venus-VGAT mice were generated as described (Wang et al., 2009). These mice express Venus fluorescent protein (a yellow fluorescent protein variant developed by Dr. Atsushi Miyawaki at RIKEN in Wako, Japan) under control of the vesicular GABA transporter. This leads to Venus expression in virtually every GABAergic and glycinergic neuron throughout the brain (Wang et al., 2009). A breeding colony was established at the University of New Mexico Health Sciences Center Animal Resource Facility. Mice were maintained as heterozygous for the Venus-VGAT transgene (hereafter referred to as Venus-VGAT^{+}), and offspring were group-housed with littermates of the same sex at 22°C on a reverse 12-hr light/dark cycle (lights on at 2000 hours) with standard chow and water available *ad libitum*.

Breeding

60 to 180 day old wild type C57BL/6 or Venus-VGAT^{+} female mice were paired with a Venus-VGAT^{+} male or a wild type C57BL/6 male breeder, respectively. After pregnancy was evident, the male mice were removed from the cage. Following parturition, postnatal day (P) 1-P2 pups were screened for the presence of the Venus-VGAT transgene by exposing

them to 460-495 nm wavelength light and observing yellow fluorescence emitted by the brain with a 520-550 nm filter using a “miner’s lamp” (Biological Laboratory Equipment Maintenance and Service LTD, Budapest, Hungary).

Tissue collection

To collect tissue, mice were anesthetized with ketamine (250 mg/kg i.p.) and perfused transcardially with 32°C phosphate buffered saline (PBS) containing procaine hydrochloride (1g/L; Sigma-Aldrich, St. Louis, MO) and heparin (1USP unit/mL; Sagent Pharmaceuticals, Schaumburg, IL) for 2 min, followed by room-temperature (~21°C) 4% paraformaldehyde (PFA; Sigma-Aldrich) in PBS for 2 min, then with ice cold 4% PFA in PBS for 5 min. Extracted brains were incubated in 4% PFA in PBS for 48 h at 4°C with gentle shaking, then cryoprotected in 30% sucrose in PBS for 48 h. Brains were embedded in Optimal Cutting Temperature compound (Fisher Healthcare, Houston, TX) and frozen in isopentane (Avantor Performance Materials, Center Valley, PA) cooled with a bath of 95% EtOH and dry ice. Brains were kept frozen at −80°C until sectioned in the parasagittal plane on a cryostat (Microm Model HM 505E, Waldorf, Germany) at 50 μm. Floating sections were kept at −20°C in freezing medium (0.05 M phosphate buffer pH 7.4, 25% glycerol and 25% ethylene glycol).

Experiment 1: Analysis of activated caspase-3 expression in mouse hippocampal interneurons following a single dose of EtOH during the third trimester equivalent of human gestation

Single P7 EtOH vapor chamber exposure—Venus-VGAT^{+} pups along with the dam were randomly assigned to one of two treatment groups. Specifically, mice were exposed to either vaporized EtOH or air for 4 h during a single exposure session on P7. This developmental time point in the mouse takes place during the equivalent of the third trimester of human gestation (West, 1987). EtOH vapor or air exposures took place in custom built EtOH vapor chambers described previously (Morton et al., 2014). EtOH vapor concentrations were measured using a breathalyzer (Intoximeters, St. Louis, MO) and were 7-8 g/dl. Animals were perfused and brains were collected 8 h after the end of the 4-h vapor chamber exposure, which previous research has determined is the optimal time point for observing activated caspase-3 expression after P7 EtOH exposure (Olney et al., 2002). To measure blood EtOH concentrations (BECs) in pups, a separate litter of Venus-VGAT^{+} pups were subjected to the above-described vapor chamber exposure paradigm but were anesthetized with isoflurane immediately following the 4-h vapor chamber exposure. Pups were decapitated and trunk blood collected. BECs were measured using an alcohol dehydrogenase-based assay described previously (Galindo and Valenzuela, 2006), expressed as mg/dl. For reference, the legal BEC limit for driving in the United States is 80 mg/dl.

Activated caspase-3 immunohistochemistry and exhaustive cell counting—Activated caspase-3 expression was examined using immunohistochemistry as described previously (Topper et al., 2015), with small alterations. Briefly, eight parasagittal sections 250 μm apart through the dorsal hippocampus of 5 air-exposed and 5 EtOH-exposed P7 brains were chosen for immunohistochemistry. The landmark for the starting medial section was the first section in which the superior and inferior granule cell layer blades of the dorsal

dentate gyrus could be clearly identified. The landmark for the most lateral section was the last section before the dorsal and ventral granule cell layers joined together. This is roughly equivalent to image 227 to image 315 in the atlas of the developing P7 mouse brain provided by the Allen Brain Institute (please see Web References for URL). Sections were incubated in PBS containing 1% bovine serum albumin (Sigma-Aldrich), 0.2% Triton X-100 (Sigma-Aldrich), and 5% donkey serum (Jackson ImmunoResearch, West Grove, PA) for 2 h. Sections were then incubated with a 1:400 dilution of anti-cleaved caspase 3 antibody (Cell Signaling cat #9661, Danvers, MA) for 72 h at 4°C with gentle shaking. Donkey anti-rabbit IgG Alexa Fluor 555 antibody (cat# A-31572, ThermoFisher, Waltham, MA) was then applied to the tissue sections at a 1:1000 dilution for 2 h, and then rinsed with PBS. Tissue sections were next incubated with 600 nM 4′6-diamidino-2-phenylindole hydrochloride (DAPI, Sigma-Aldrich) solution for 20 min, rinsed in PBS, mounted on Superfrost plus slides (VWR, Radnor, PA), coverslipped with Vectashield mounting media (Vector Laboratories, Burlingame, CA), and sealed with nail polish.

Sections were imaged on a Nuance spectral imaging system (PerkinElmer, Hopkinton, MA) as described previously (Noor et al., 2017) at the University of New Mexico Health Sciences Center Fluorescence Microscopy Shared Resource. Images of P7 hippocampi were acquired using a 10× objective on a Nikon TE-200 U inverted fluorescence microscope. High magnification images were taken using a 40× objective. Uneven field illumination and other artifacts were removed using flat-field correction to generate a uniform illumination during image acquisition. Pure labels for each fluorophore were created by generating a spectral library from single-labeled control slides and an unlabeled, autofluorescence slide. The computed spectrum for each label was produced by subtracting the autofluorescence from the single-labeled spectrum. Experimental images were then un-mixed using the computed single-labeled spectrums to obtain composite images containing the labels of interest. Images of the hippocampus that were larger than the field of view were stitched together using the Pairwise Stitching plugin (Preibisch et al., 2009) in NIH Image J software (Schneider et al., 2012). An experimenter blinded to the experimental conditions then exhaustively counted the number of Venus-VGAT positive cells (green channel), the number of activated caspase-3 positive cells (red channel), and the number of colocalized activated caspase-3 positive Venus-VGAT cells in each section and each region of the hippocampus (CA1, CA3, granule cell layer (GCL), and the hilus). A separate experimenter performed a separate count of a subset of sections to confirm the first experimenter's accuracy (results were within 15% of each other). The number of DAPI nuclei were estimated in each tissue section and hippocampal region using the Find Maxima process in Image J.

In P7 animals, we did not use unbiased stereology due to the relatively small number of cells that were positive for either activated caspase-3 or both activated caspase-3 and Venus in hippocampal regions of interest. Under these conditions, we would have been unable to obtain an acceptable Gundersen coefficient of error by using the optical fractionator method. Therefore, we opted to exhaustively count the number of cells in every 8^{th} section, similar to a procedure that has been previously used to characterize the developmental effect of ethanol on cortical interneurons (Smiley et al., 2015).

Experiment 2: Analysis of long-term interneuron viability using unbiased stereology in mice exposed to EtOH during the third trimester equivalent of human gestation

P2-P9 third trimester-equivalent vapor chamber exposure—Venus-VGAT^{+} mouse pups along with their dam were randomly assigned to either air or EtOH exposure conditions as described in Experiment 1, with the following modifications. Animals were exposed to air or EtOH for 4 h/day from P2-P9, which encompasses the majority of the third trimester-equivalent period of human gestation (West, 1987). Vapor chamber EtOH levels were gradually increased as follows: 3-4 g/dl at P2-3, 5-6 g/dl at P4-5 and 7-8 g/dl at P6-9. BECs were measured (as described above) midway through the exposure paradigm at P5 in a separate cohort of animals. Pups were weaned at P21, and group-housed with littermates of the same sex. On P90, air and EtOH exposed mice were cardiacally-perfused and brains collected, as described above.

Assessment of pup development

To assess acquisition of developmental milestones, pups from each vapor chamber-exposure condition were monitored daily to determine what postnatal day they acquired a righting reflex, opened their eyes, displayed an auditory startle reflex, or displayed an ear twitch in response to tactile stimulation (Chi et al., 2016; Wu et al., 1997). Pups were also weighed on P1, P5, P9, and P16 to monitor development. Maternal care was assessed following vapor chamber exposure on P2 and P5 by displacing a pup from the nest and measuring how long it took the dam to navigate to and retrieve the pup, as well as measuring the latency to rebuild a disrupted nest.

Unbiased Stereology

Stereological estimation of total Venus^{+} interneurons was performed on P90 animals. Sections used for stereology were washed 4 times for 5 min with PBS, and then incubated with 600 nM DAPI in PBS for 20 min. Sections were again washed 4X in PBS before being mounted on Superfrost plus slides and coverslipped with Vectashield mounting media. Coverslips were sealed around the edges with clear nail polish. Stereology was performed by means of the optical fractionator probe of unbiased stereological cell counting method using Stereoinvestigator software (Microbrightfield Bioscience, Williston, VT). Sections were imaged using an Olympus IX-81 DSU spinning disk confocal microscope at the University of New Mexico Health Sciences Center Fluorescence Microscopy Shared Resource. Every 5th parasagittal section through the dorsal hippocampus (lateral 0.36 to 2.52 mm according to the Paxinos adult mouse brain atlas (Paxinos and Franklin, 2013)) was counted. If any section was torn or damaged, the closest intact section was used instead. Contours were manually drawn around the following hippocampal regions: CA1, CA3, GCL, and the hilus. For all regions examined, the dissector height was 12 μm with a 4 μm guard zone. Venus-VGAT populations were estimated in the CA1 and CA3 using a 70 × 70 μm counting frame and a 140 × 140 μm sampling grid. For the GCL and hilus, Venus expressing cells were counted using a 70 × 70 μm counting frame with a 100 × 100 μm sampling grid. For all cell counts, the Gundersen coefficient of error was less than the recommended upper limit value of 0.10 (Gundersen et al., 1999). The volumes of CA1, CA3, GCL and the hilus were

estimated using the contours drawn around the hippocampal subregions as reported by the planimetry output from StereoInvestigator.

Statistical analyses

Data are presented as mean ± SEM in all cases. Statistical analyses were performed using SPSS version 24 for Windows (IBM, Armonk, NY) and Prism 7 (GraphPad Software, San Diego, CA). An alpha of 0.05 was adopted for all analyses. Differences in the 2D area, DAPI nuclei count, Venus$^+$ cell count, activated caspase-3$^+$ cell count, colocalized Venus$^+$/caspase-3$^+$ cell count, percentage of caspase-3$^+$ cells per total DAPI count, and the percentage of caspase-3$^+$ interneurons between vapor chamber exposure conditions in each hippocampal subregion were analyzed using repeated measures ANOVA. The eight levels of the within-subjects factor were the medial-lateral parasagittal tissue sections, and the between subjects factor was the vapor chamber exposure condition. Statistical values reported from the repeated measures ANOVA include F ratio, p value, and effect size reported as partial eta squared (η_p^2). For any repeated measures that violated assumptions of sphericity, Greenhouse-Geisser corrected p values and F ratios are reported. Within-subjects effects of medial to lateral tissue section, and interaction of medial to lateral tissue section with vapor chamber exposure condition are reported for the percentage of total cells with activated caspase-3 and the percentage of total interneurons with activated caspase-3. Pup weights were analyzed using a two-way ANOVA with age and vapor chamber exposure condition as the fixed factors. Acquisition of developmental milestones and maternal care measures were analyzed using two-tailed, unpaired t-tests. For P90 unbiased stereology experiments, data were first analyzed using a univariate factorial ANOVA using either volume or Venus$^+$ cell count as the dependent variable, with vapor chamber exposure condition, hippocampal subregion, and sex as the fixed factors. Results were then analyzed with an univariate ANOVA within each hippocampal subregion, again using either volume or Venus$^+$ cell count as the dependent variable, and vapor chamber exposure condition and sex as the fixed factors. To examine the effect of vapor chamber exposure condition in each hippocampal subregion within level of sex, post-hoc multiple comparisons were run to further explore significant exposure effects and Sidak adjusted p-values are presented. Hedges' g effect sizes are reported for multiple comparisons and t-tests to allow for comparison of the size of differences between group means (Hedges and Olkin, 1985). Hedges' g is analogous to Cohen's d (Cohen, 1988) for effect size, but corrects for bias caused by using smaller sample sizes (Cumming, 2012; Lakens, 2013). Standard benchmarks for small ($\eta_p^2 = 0.01$; $g = 0.2$), medium ($\eta_p^2 = 0.06$; $g = 0.5$); and large ($\eta_p^2 = 0.14$; $g = 0.8$) effect sizes can be inferred based on the work of Cohen (1988).

RESULTS

Experiment 1: EtOH exposure at P7 activated apoptotic pathways in hippocampal interneurons

To ascertain if hippocampal interneurons are vulnerable to EtOH during early postnatal development, mouse pups along with their dams were exposed to a single air or EtOH vapor chamber exposure session at P7. BECs were collected in a separate cohort of pups immediately following the 4-h vapor chamber exposure paradigm. The mean BEC in pups

was 297.2 ± 19.0 mg/dl (n = 5 pups). Eight hours after the cessation of the vapor chamber exposure session, brains were collected from pups and processed to examine cleaved caspase-3 expression as a marker of activation of apoptotic pathways (representative images from an EtOH-exposed animal appear in Figure 1A–G). The area, number of DAPI nuclei, number of interneurons, number of cells with activated caspase-3, number of caspase-3 positive interneurons, the percentage of total cells with activated caspase-3, and the percentage of total interneurons with activated caspase-3 were measured in each medial to lateral section through the following regions of the dorsal hippocampus: the hilus of the dentate gyrus, the GCL, CA1, and CA3. Data from the combined hippocampal regions are also presented. Results were analyzed using a repeated measures ANOVA, with medial to lateral parasagittal section as the within subjects measure, and vapor chamber exposure condition as the between subjects measure.

The total area of each hippocampal region was not affected by the single EtOH exposure at P7 (Figure 1H, hilus $F(1,8) = 0.382$, $p = 0.55$, $\eta_p^2 = 0.046$; GCL $F(1,8) = 0.256$, $p = 0.63$, $\eta_p^2 = 0.031$; CA1 $F(1,8) = 1.349$, $p = 0.28$, $\eta_p^2 = 0.144$; CA3 $F(1,8) = 2.948$, $p = 0.12$, $\eta_p^2 = 0.269$; combined regions $F(1,8) = 0.186$; $p = 0.68$; $\eta_p^2 = 0.085$). There was also no effect of EtOH exposure on the number of DAPI nuclei within each hippocampal region (Figure 1I, hilus $F(1,8) = 0.433$, $p = 0.53$, $\eta_p^2 = 0.051$; GCL $F(1,8) = 0.171$, $p = 0.69$, $\eta_p^2 = 0.021$; CA1 $F(1,8) = 1.349$, $p = 0.28$, $\eta_p^2 = 0.144$; CA3 $F(1,8) = 0.557$, $p = 0.48$, $\eta_p^2 = 0.065$; combined regions $F(1,8) < 0.001$, $p > 0.99$, $\eta_p^2 < 0.001$). Likewise, there was no effect of vapor chamber exposure condition on the total number of interneurons in any region (Figure 1J, hilus $F(1,8) = 0.324$, $p = 0.32$, $\eta_p^2 = 0.121$; GCL $F(1,8) = 0.004$, $p = 0.95$, $\eta_p^2 < 0.001$; CA1 $F(1,8) = 2.345$, $p = 0.16$, $\eta_p^2 = 0.227$; CA3 $F(1,8) = 1.170$, $p = 0.31$, $\eta_p^2 = 0.128$; combined regions $F(1,8) = 1.788$, $p = 0.22$, $\eta_p^2 = 0.183$).

Exposure to vaporized EtOH at P7 caused caspase-3 activation throughout the entire hippocampus compared to air-exposed controls (Figure 1K). In the hilus, EtOH exposure led to a roughly eight-fold increase in the number of cells undergoing apoptosis compared to air controls ($F(1,8) = 14.707$, $p = 0.005$, $\eta_p^2 = 0.648$). There was also a 5-fold increase in activated caspase-3^+ cells in the GCL ($F(1,8 = 37.946$, $p < 0.001$, $\eta_p^2 = 0.826$), an 8-fold increase in the CA1 ($F(1,8) = 11.615$, $p = 0.009$, $\eta_p^2 = 0.592$) and a 4-fold increase in the CA3 ($F(1,8) = 28.414$, $p = 0.001$, $\eta_p^2 = 0.780$). In the combined hippocampal subregions examined in this study, there was a 6-fold increase in activated caspase-3^+ cells in EtOH-exposed animals compared to air-exposed controls ($F(1,8) = 18.092$, $p = 0.003$, $\eta_p^2 = 0.693$).

We also measured activated caspase-3 expression as a percentage of the total DAPI positive cells in each hippocampal subregion (Figure 1L). Using this measure of activated caspase-3 expression, there was again an effect of vapor chamber exposure condition in every hippocampal region examined. In the hilus, EtOH exposure activated caspase-3 in approximately 0.98% of all cells, compared to air exposed animals in which only 0.13% of all cells expressed activated caspase-3 ($F(1,8) = 13.666$, $p = 0.006$, $\eta_p^2 = 0.631$). EtOH exposure activated caspase-3 in 0.16% of GCL cells vs. 0.03% in the air exposure group ($F(1,8) = 33.095$, $p < 0.001$, $\eta_p^2 = 0.805$), in 0.52% of CA1 cells vs. 0.06% in the air exposure group ($F(1,8) = 11.427$, $p = 0.010$, $\eta_p^2 = 0.588$), and in 0.39% of CA3 cells vs. 0.10% in the air exposure group ($F(1,8) = 29.596$, $p = 0.001$, $\eta_p^2 = 0.787$). In combined

regions, EtOH exposure activated caspase-3 in 0.45% of all cells, compared to 0.07% activation in air-exposed animals ($F(1,8) = 19.092$, $p = 0.002$, $\eta_p^2 = 0.704$).

We next ascertained if a single EtOH exposure at P7 activated apoptotic pathways in hippocampal interneurons by measuring the number of Venus + cells expressing activated caspase-3 in each of the hippocampal regions (Figure 1M). In each region of the hippocampus, EtOH exposure caused a significant increase in the number of activated caspase-3 positive interneurons compared to air controls (hilus $F(1,8) = 11.751$, $p = 0.009$, $\eta_p^2 = 0.595$; GCL $F(1,8) = 8.641$, $p = 0.019$, $\eta_p^2 = 0.519$; CA1 $F(1,8) = 12.650$, $p = 0.007$, $\eta_p^2 = 0.686$; CA3 $F(1,7) = 14.664$, $p = 0.006$, $\eta_p^2 = 0.677$l; combined regions $F(1,7) = 14.910$, $p = 0.006$, $\eta_p^2 = 0.613$). We also measured the number of the caspase-3 postitive interneurons as a percentage of the total number of Venus+ cells (Figure 1N). We observed a significant effect of vapor chamber exposure condition on the percentage of interneurons with activated caspase-3 in every hippocampal region. In the hilus, EtOH exposure activated caspase-3 in 5.53% of all interneurons, compared to 0.39% activation in interneurons of air-exposed animals ($F1,8) = 12.678$, $p = 0.007$, $\eta_p^2 = 0.613$). EtOH exposure activated caspase-3 in 2.24% of GCL interneurons vs. 0.22% in the air exposure group ($F1,8) = 8.150$, $p = 0.021$, $\eta_p^2 = 0.505$), in 3.28% of CA1 interneurons vs. 0.19% in the air exposure group ($F(1,8) = 13.198$, $p = 0.007$, $\eta_p^2 = 0.623$), and in 2.95% of CA3 interneurons vs. 0.18% in the air exposure group ($F(1,8) = 15.905$, $p = 0.004$, $\eta_p^2 = 0.665$. In combined regions, EtOH exposure activated caspase-3 in 3.47% of all interneurons, compared to 0.22% activation in all interneurons of air-exposed animals.

In the hilus of EtOH exposed animals, roughly 70% of all cleaved caspase-3 positive cells were interneurons. In the other regions of the hippocampus, cleaved caspase-3 positive interneurons also comprised large proportions of the total number of apoptotic cells in EtOH exposed animals (GCL 40%, CA1 45%, and CA3 36%). In all regions of the hippocampus examined, interneurons comprised 45% of all cleaved caspase-3 positive cells. These results indicate that interneurons of the hippocampus are particularly vulnerable to the effects of developmental EtOH exposure.

Using our within-subjects study design, we also examined the effect of medial to lateral tissue section and vapor chamber exposure condition on the percentage of activated caspase-3 positive cells and the percentage of activated caspase-3 positive interneurons in the dorsal hippocampus of P7 mice. Within subjects, there was no effect of medial to lateral tissue section on the percentage of activated caspase-3 positive cells in the hilus (Figure 2A, section $F(2.362,18.897) = 1.434$, $p = 0.26$, $\eta_p^2 = 0.152$; section*exposure $F(2.362,18.897) = 2.113$, $p = 0.14$, $\eta_p^2 = 0.209$) or in the GCL (Figure 2B, section $F(7,56) = 1.207$, $p = 0.31$, $\eta_p^2 = 0.131$; section*exposure $F(7,56) = 1.521$, $p = 0.18$, $\eta_p^2 = 0.160$). In the CA1 (Figure 2C section $F(2.178,17.422) = 3.999$, $p = 0.034$, $\eta_p^2 = 0.333$; section*exposure $F(2.178,17.422) = 3.969$, $p = 0.035$, $\eta_p^2 = 0.332$), the CA3 (Figure 2D, section $F(2.932,23.453) = 4.596$, $p = 0.012$, $\eta_p^2 = 0.365$; section*exposure $F(2.932,23.453) = 1.574$, $p = 0.22$, $\eta_p^2 = 0.164$), and the combined hippocampal regions (Figure 2E, section $F(7,56) = 10.482$, $p < 0.001$, $\eta_p^2 = 0.567$; section*exposure $F(7,56) = 7.579$, $p < 0.001$, $\eta_p^2 = 0.486$) there was a higher percentage of cells with activated caspase-3 in medial sections compared to lateral sections. There was no effect of medial to lateral tissue section on the percentage

of activated caspase-3 positive interneurons in the hilus (Figure 2F, section $F(2.187,17.496) = 0.663$, $p = 0.54$, $\eta_p^2 = 0.077$; section*exposure $F(2.187,17.496) = 1.099$, $p = 0.36$, $\eta_p^2 = 0.121$) the GCL (Figure 2G, section $F(2.455,19.638) = 0.452$, $p = 0.68$, $\eta_p^2 = 0.053$; section*exposure $F(2.455,19.638) = 0.669$, $p = 0.55$, $\eta_p^2 = 0.077$) or the CA1 (Figure 2H, section $F(1.788,14.306) = 3.148$, $p = 0.078$, $\eta_p^2 = 0.282$; section*exposure $F(1.788,14.306) = 3.489$, $p = 0.062$, $\eta_p^2 = 0.304$). The percentage of activated caspase-3 positive interneurons was higher in medial sections compared to lateral sections in the dorsal CA3 (Figure 2I, section $F(2.028,16.227) = 11.112$, $p = 0.001$, $\eta_p^2 = 0.581$; section*exposure interaction $F(2.028,16.227) = 8.259$, $p = 0.003$, $\eta_p^2 = 0.508$) and the combined hippocampal regions (Figure 2J, section $F(7,56) = 26.671$, $p < 0.001$, $\eta_p^2 = 0.770$; section*exposure interaction $F(7,56) = 16.684$, $p < 0.001$, $\eta_p^2 = 0.676$).

Experiment 2: Third trimester-equivalent EtOH exposure causes a long-term decrease in hippocampal interneuron numbers

To model EtOH exposure during the third trimester equivalent of human gestation, Venus-VGAT+ litters along with their dams were exposed to either air or vaporized EtOH from P2 to P9. BECs were measured from a separate cohort of pups midway through the exposure paradigm at P5. The mean BEC at P5 was 221.6 ± 18.3 mg/dl (n = 6 litters). One of the goals of our study was to determine if our developmental EtOH exposure paradigm resulted in any significant changes in normal pup development, which may confound interpretation of subsequent analyses. Mice were weighed before (P1), during (P5 and P9), and after (P16) the vapor chamber exposure paradigm to determine if EtOH exposure had a significant effect on normal pup growth in Venus-VGAT$^+$ mice (Figure 3A). There were no differences in pup weights between vapor chamber exposure conditions (exposure $F(1,64) = 0.016$, $p = 0.90$, $\eta_p^2 < 0.001$; age $F(3,64) = 282.682$, $p < 0.001$, $\eta_p^2 = 0.930$; age*exposure $F(3,64) = 0.257$, $p = 0.86$, $\eta_p^2 = 0.012$). We also obtained other measures to ascertain if EtOH exposure has a significant effect on the normal trajectory of pup development. Six litters of pups from each vapor chamber exposure condition were monitored daily to determine the postnatal day that they acquired developmental milestones (Figure 3B). There were no effects of vapor chamber exposure condition on the day at which pups achieved the following milestones: surface righting ($t(10) = 0.36$, $p = 0.73$, $g = 0.20$), open field traversal ($t(10) = 0.32$, $p = 0.76$, $g = 0.17$), eye opening ($t(10) = 0.66$, $p = 0.53$, $g = 0.53$), auditory startle ($t(10) = 1.21$, $p = 0.25$, $g = 0.65$), and ear twitch ($t(10) = 0.55$, $p = 0.59$, $g = 0.29$).

A separate factor that could have influenced pup development and confound interpretation of subsequent results concerns maternal care following exposure to EtOH in the vapor chambers. To determine if EtOH exposure had a significant effect on how well dams cared for their pups, we performed three separate measurements on developmental days P2 and P5. For the first two measurements, we assessed how long it took dams to navigate to pups displaced from their nests, and then how long it took the dams to return the pups to the nest. The other aspect of maternal care that was measured concerned how long it took a dam to rebuild a disrupted nest. There were no differences between vapor chamber exposure conditions at either P2 or P5 for: the latency to navigate to a displaced pup (P2 $t(10) = 0.36$, $p = 0.73$, $g = 0.19$; P5 $t(10) = 0.17$, $p = 0.87$, $g = 0.09$), the latency to retrieve a displaced pup (P2 $t(10) = 0.10$, $p = 0.92$, $g = 0.05$; P5 $t(10) = 0.64$, $p = 0.53$, $g = 0.34$), or the latency

to rebuild a disrupted nest (P2 t(10) = 1.29; p = 0.23, g = 0.69; P5 t(10) = 1.20; p = 0.26, g = 0.64) (Table 1). These findings indicate that subsequent significant effects discussed in this manuscript are not due to deficits in maternal care caused by EtOH vapor chamber exposure.

After determining that interneurons of the hippocampus are vulnerable to the effects of EtOH exposure during the third trimester equivalent of human gestation, the next goal of this study was to ascertain if caspase 3 activation in interneurons following EtOH exposure translates into a loss of hippocampal interneurons in the long-term. To accomplish this goal, we exposed Venus-VGAT$^+$ mice of both sexes to air or EtOH from P2 to P9 in vapor chambers, and collected brains at P90. Sections throughout the entire dorsal hippocampus were collected and counterstained with DAPI, and unbiased stereology was utilized to count the total number of surviving Venus-VGAT positive interneurons in, and the total volume of, each of the hippocampal regions of interest (representative images from a P90 air-exposed brain appear in Figure 4A–C).

Data collected from unbiased stereology was first analyzed using a factorial, univariate ANOVA using either volume or interneuron cell count as the dependent variable, and vapor chamber exposure condition, sex, and hippocampal subregion as the fixed factors. Using this approach, there was a single significant effect of hippocampal subregion on the volume measured, which was expected because the different hippocampal subregions have different morphological characteristics. There was no effect of vapor chamber exposure condition or sex on volume, and no significant interactions between any of the fixed factors. There were significant effects of exposure (F(1,112) = 31.443, p < 0.001, η_p^2 = 0.219), sex (F(1,112) = 8.959, p = 0.003, η_p^2 = 0.074) and region on the number of Venus$^+$ interneurons measured. There were no significant interactions of any of the fixed factors on interneuron counts.

We next analyzed the data separately within each hippocampal subregion, using vapor-chamber exposure condition and sex as the fixed factors. In addition, we also examined the effect of vapor chamber exposure condition in each hippocampal subregion within level of sex using post hoc multiple comparisons analyses. There were no long-term consequences of P2-P9 EtOH exposure on the volume of the hilus (Figure 4D, sex*exposure F(1,28) = 0.120, p = 0.73 η_p^2 = 0.004; sex F(1,28) = 0.421, p = 0.52, η_p^2 = 0.015; exposure F(1,28) = 1.788, p = 0.19, η_p^2= 0.060), on the volume of the CA1 (Figure 4F, sex*exposure F(1,28) = 0.646, p = 0.43, η_p^2 = 0.023; sex F(1,28) = 0.737, p = 0.40, η_p^2 = 0.026; exposure F(1,28) = 2.250, p = 0.15, η_p^2= 0.074), on the volume of the CA3 (Figure 4G, sex*exposure F(1,28) = 1.185, p = 0.29, η_p^2 = 0.41; sex F(1,28) = 1.999, p = 0.17, η_p^2 = 0.067, exposure F(1,28) = 0.004, p = 0.95, η_p^2< 0.001), or on the volume of the combined regions (Figure 4H, sex*exposure F(1,28) = 0.613, p = 0.43, η_p^2 = 0.021; sex F(1,28) = 0.915, p = 0.35, η_p^2 = 0.032; exposure F(1,28) = 2.353, p = p.14, η_p^2 = 0.078). P2-P9 EtOH exposure did cause a significant decrease in volume in the GCL at P90 (Figure 4E, sex*exposure F(1,28) = 0.550, p = 0.46, η_p^2 = 0.019; sex F(1,28) = 0.359, p = 0.55, η_p^2 = 0.013; exposure F(1,28) = 5.265, p = 0.029, η_p^2 = 0.158). This effect was not significant within sex following post hoc multiple comparison analysis (male p = 0.080, g = 1.01; female p = 0.48, g = 0.52).

Third trimester-equivalent EtOH exposure had a number of effects on the population of hippocampal interneurons at P90. In the hilus, EtOH exposure decreased interneuron

numbers by 15.1% compared to air-exposed animals (Figure 4I, sex*exposure F(1,28) = 0.65, p = 0.43, η_p^2 = 0.023; sex F(1,28) = 0.12, p = 0.73, η_p^2 = 0.004; exposure F(1,28) = 6.89, p = 0.014, η_p^2 = 0.197). Within sex, EtOH exposure caused a significant decrease in hilar interneuron number in males (19.2% decrease, p = 0.043, g = 1.08), but not in females (p = 0.38, g = 0.65). In the GCL, females had a larger population of interneurons compared to males. EtOH exposure significantly reduced the population of interneurons in the GCL by 15.8% (Figure 4J, sex*exposure F(1,28) = 0.14, p = 0.71, η_p^2 = .005; sex F(1,28) = 4.52, p = 0.043, η_p^2= 0.139; exposure F(1,28) = 7.56, p = 0.010, η_p^2 = 0.213). However, there was no significant effect of EtOH exposure on the population of interneurons within sex in the GCL at P90 (male p = 0.070, g = 0.99; female p = 0.20, g = 0.84). EtOH vapor chamber exposure significantly decreased surviving interneuron numbers in the CA1 by 12.7% (Figure 4K, sex*exposure F(1,28) = 0.21, p = 0.65, η_p^2 = 0.007; sex F(1,28) = 3.62, p = 0.067, η_p^2= 0.115; exposure F(1,28) = 11.52, p = 0.0021, η_p^2 = 0.292). Within sex in the CA1, there was a significant effect of vapor chamber exposure condition in males (14.8% decrease, p = 0.022, g = 1.16) that was absent in females (p = 0.092, g = 1.12). In the CA3, EtOH exposure significantly decreased the number of interneurons by 11.1% compared to air-exposed animals. Females also had a larger population of interneurons compared to males in the CA3 regardless of vapor chamber exposure condition (Figure 4L, sex*exposure F(1,28) = 0.77, p = 0.39, η_p^2 = 0.027; sex F(1,28) = 4.92, p = 0.035, η_p^2= 0.149; exposure F(1,28) = 6.23, p = 0.019, η_p^2 = 0.182). Within sex in the CA3, there was only an effect of vapor chamber exposure in males (15.5% decrease, p = 0.048, g = 0.99; female p = 0.46, g = 0.64). When the results from each of the hippocampal regions were combined, ethanol exposure resulted in an overall decrease in the population of interneurons by 13.2% (Figure 4M, sex*exposure F(1,28) = 0.609, p = 0.44, η_p^2 = 0.021; sex F(1,28) = 3.839, p = 0.060, η_p^2 = 0.120; exposure F(1,28) = 13.443, p = 0.001, η_p^2 = 0.324). Within sex for the combined hippocampal regions, there was a significant effect of vapor chamber exposure condition on interneuron counts in males (16.4% decrease, p = 0.008, g = 1.28), with no significant effect in females (p = 0.099, g = 1.20). These results demonstrate that third trimester-equivalent EtOH exposure has a lasting impact on the surviving population of hippocampal interneurons, and that males are particularly vulnerable to this effect.

DISCUSSION

This study provides evidence that third-trimester equivalent EtOH exposure results in a long-term reduction in hippocampal interneuron populations throughout the hippocampus. During the third trimester equivalent of human gestation, a single dose of EtOH caused a robust activation of apoptosis throughout the hippocampus as evidenced by increased cleaved caspase-3 expression, replicating results previously seen in other studies (Camargo Moreno et al., 2017; Ikonomidou et al., 2000; Ogievetsky et al., 2017; Olney et al., 2002). As was seen in the study by Ogievetsky et al, the population of interneurons undergoing apoptosis was significantly elevated in all the hippocampal regions that were examined. In the hippocampal regions measured in this study, approximately 0.45% of cells expressed activated caspase-3 after exposure to EtOH on P7. Of those cells, almost half were interneurons. Interneurons of the hilus of the dentate gyrus seemed to be particularly vulnerable to the effects of developmental EtOH exposure. Degenerating interneurons

accounted for roughly 70% of all the activated caspase-3 positive cells in the hilus. In the other hippocampal regions examined, at least 36% of the degenerating cells were interneurons. Given that roughly 20% of cells in the hippocampus are interneurons (Freedman et al., 1993; Olbrich and Braak, 1985), these results suggest that hippocampal interneurons are more susceptible than other cell types of the hippocampus to the deleterious effects of third trimester-equivalent EtOH exposure. Based on these facts, it is likely that in previous studies that examined how developmental ethanol exposure activated apoptotic neurodegeneration, a large proportion of degenerating neurons in the hippocampus were interneurons (Camargo Moreno et al., 2017; Ikonomidou et al., 2000; Olney et al., 2002). It is improbable that interneurons had already degenerated and lost Venus fluorescence before we counted their populations, as the number of Venus+ cells and the total number of DAPI nuclei were not significantly different between exposure conditions in any of the hippocampal regions examined. Cells in the medial sections of the dorsal CA1, CA3 and combined hippocampal regions were more vulnerable to EtOH exposure than more lateral sections. The reason for this vulnerability gradient is unknown and is an interesting topic for further study. Mice were only exposed to a single EtOH vapor chamber exposure to assess activation of the apoptotic cell death pathway in this study, paralleling the methodology of Olney et al. (2002), who characterized how postnatal EtOH exposure causes apoptotic neurodegeneration. Olney et al. chose P7 as their exposure time point based on the fact that this is the day when the peak of synaptogenesis occurs (Semple et al., 2013). It remains unknown, however, as to what particular postnatal day hippocampal interneurons are the most susceptible to EtOH exposure. GABAergic signaling on postsynaptic neurons in the rodent brain progressively changes from depolarizing to hyperpolarizing during the first postnatal week, a well-characterized phenomenon known as the “GABA switch” (Ben-Ari, 2014; Valeeva et al., 2013). The excitatory actions of GABA during early development have been proposed to be critical for synchronization of hippocampal network activity (Ben-Ari et al., 2012), therefore, specific loss of GABAergic interneurons by developmental EtOH exposure could have profound impacts on the development and function of the hippocampus and interconnected brain areas depending on the precise timing of when apoptotic neurodegeneration takes place (Galindo et al., 2005; Kajimoto et al., 2016; Rodriguez et al., 2016a; Wilson et al., 2011).

Activated caspase-3 expression, in this study, was used as a marker of apoptotic neurodegeneration. The role of caspase-3 in both the intrinsic and extrinsic apoptotic cell-death pathways has been well studied. For both of these apoptotic pathways, upstream signaling events lead to activation of caspase-3, which in turn activates various endonucleases and proteases (for review, see Elmore, 2007). This results in degradation of chromosomal DNA, nuclear and cytoskeletal proteins, and ultimately leads to the formation of apoptotic bodies that are engulfed by phagocytic cells (Hochreiter-Hufford and Ravichandran, 2013). Caspase-3 activation, however, has other functional roles in neurons unrelated to apoptosis (D’Amelio et al., 2010). Long-term depression of synaptic activity is dependent on caspase-3 activity, which regulates dendritic spine density and dendritic morphology without causing apoptotic cell death (Erturk et al., 2014). Other groups have proposed that caspase-3 is required for long-term potentiation in the CA1 of the hippocampus (Gulyaeva et al., 2003), and have found that inhibition of caspase-3 activity is

detrimental to learning and memory processes (Huesmann and Clayton, 2006; Stepanichev et al., 2005). Given that previous research examining the effects of P7 EtOH exposure using analogous exposure paradigms to ours have found activated apoptosis in the hippocampus by other methodologies, including silver-stain (Ikonomidou et al., 2000) and TUNEL staining (Camargo Moreno et al., 2017), it is likely that activated caspase-3 positive cells observed in this study are undergoing apoptotic neurodegeneration.

At P90, there was only a single effect of third trimester-equivalent EtOH exposure on hippocampal volume, which was a small reduction of GCL layer volume independent of sex. Reduced GCL volume at P90 could reflect reduced adult hippocampal granule cell neurogenesis, which has been shown to be caused by developmental EtOH exposure (Hamilton et al., 2011; Klintsova et al., 2007). This reduction in GCL volume may also be due to reduced GCL dendritic arborization caused by EtOH exposure (Staples et al., 2015). While there was only one effect of developmental exposure on hippocampal volume at P90, there were numerous effects on the number of surviving hippocampal interneurons as measured by unbiased stereology. EtOH vapor chamber exposure reduced interneuron populations in the hilus, CA1, CA3, and GCL. This long-term loss of hippocampal interneurons could have many implications on hippocampal dependent behaviors. Developmental alcohol exposure has repeatedly been demonstrated to have detrimental effects on hippocampal dependent learning and memory processes (Rodriguez et al., 2016b; Varaschin et al., 2010). Hippocampal interneurons play an important role in both the consolidation (Ognjanovski et al., 2017) and retrieval (Andrews-Zwilling et al., 2012) of memory; therefore, it is possible that deficits in long-term interneuron survival observed in this study could partially explain deficits in learning and memory in animal models of FASDs. In this study, significant effects of vapor chamber exposure condition on long-term interneuron viability within level of sex were limited to male mice, with no effects observed in females. Sexually dimorphic effects are frequently observed in studies of FASDs in both human subjects and animal models (Bird et al., 2017; Hellemans et al., 2010; Thanh et al., 2014; Varlinskaya and Mooney, 2014). It is possible that sex-specific effects observed in studies of FASDs are due to expression of protective genes containing estrogen responsive elements that may compensate for the detrimental effects of EtOH exposure in females as they age into sexual maturity (Tunc-Ozcan et al., 2017).

There exist limitations of the present study that warrant further discussion. The sample sizes for both the P7 single EtOH exposure experiment, as well as for the P90 unbiased stereology study, were both relatively small. This is unlikely to affect outcomes for the P7 EtOH experiment, as results were highly significant despite the small sample size. In the P90 cell counting experiment, we used a sample size of eight animals per vapor chamber exposure condition and sex to detect differences in volume and interneuron count in hippocampal subregions. Analysis of these data resulted in significant post hoc effects in the number of interneurons for males in many of the hippocampal regions, but not females. Females did show similar trends as males with regard to these measures, so our experiments may have suffered from type II statistical error due to undersampling of subjects. Future studies will confirm the sex effects observed in this study, and if males really are more vulnerable to the effects of developmental EtOH exposure on interneuron viability.

The results from this study motivate further examination of how interneurons of the hippocampus are affected by developmental alcohol exposure. Specifically, an intriguing avenue for future research would be to study what, if any, subtype of interneuron is most susceptible to the damaging effects of EtOH. The hippocampus contains multiple subtypes of interneurons that can be classified by their morphology, physiological properties, or histological markers that they express (Maccaferri and Lacaille, 2003). The hilus of the dentate gyrus is enriched in the presence of somatostatin (Sst)-expressing interneurons, which project axons to the outer molecular layer of the dentate gyrus and synapse onto granule cell dendrites and modulate input from the perforant path (Savanthrapadian et al., 2014). These hilar perforant path associated cells have been proposed to play a role in pattern separation, an important hippocampal dependent process that allows an animal to distinguish between two similar contexts (Myers and Scharfman, 2009). In this study, some of the largest effects of alcohol exposure on interneuron loss were observed in the hilus, leading to the possibility that alcohol exposure during gestation may be particularly harmful to Sst-expressing interneurons. Deficits in spatial pattern separation have previously been described in mice exposed to EtOH during development (Kajimoto et al., 2013), and it is possible that reductions in Sst interneuron survival could be contributing to these deficits by altering network activity within the hippocampus. Future experiments using Sst-Cre driven optogenetic strategies could allow for the study of this possibility, with the caveat that these Sst-Cre mice have recently been shown to have diminished Sst expression that caused altered behavioral phenotypes and other confounding effects (Viollet et al., 2017). The death of other interneuron cell types within the hippocampus should also be taken into account when designing future studies, as other work has shown that long-term survival of PV interneurons in the CA1 is negatively affected by developmental EtOH exposure (Sadrian et al., 2014). A careful histological characterization of interneuron subtypes affected by EtOH exposure will be critical to inform the direction for future studies examining the functional outcomes of interneuron physiology in animal models of FASDs.

In conclusion, the work presented in this manuscript provides evidence for long-term consequences of developmental EtOH exposure on interneuron viability within the hippocampus. The death of hippocampal interneurons early in development could have life-long impacts on the function of the hippocampus, and may partially explain deficits in learning and memory processes observed in animal models of FASDs, as well as in humans afflicted with this disease.

Acknowledgments

Supported by NIH grants R37-AA015614 and P50-AA0022534 (CFV), as well as UNM's Undergraduate Pipeline Network (NJP). Unbiased stereology and fluorescence microscopy was carried out at the University of New Mexico & Cancer Center Fluorescence Microscopy Shared Resource, funded as detailed on: http://hsc.unm.edu/crtc/microscopy/acknowledgement.shtml. We thank Dr. Yuchio Yanagawa at the Department of Genetic and Behavioral Neuroscience at the Gunma University School of Medicine (Maebashi, Japan) for generously providing Venus-VGAT mice.

References

Andrade JP, Fernando PM, Madeira MD, Paula-Barbosa MM, Cadete-Leite A, Zimmer J. Effects of chronic alcohol consumption and withdrawal on the somatostatin-immunoreactive neurons of the rat hippocampal dentate hilus. Hippocampus. 1992; 2:65–71. [PubMed: 1364047]

Andrews-Zwilling Y, Gillespie AK, Kravitz AV, Nelson AB, Devidze N, Lo I, Yoon SY, Bien-Ly N, Ring K, Zwilling D, et al. Hilar GABAergic interneuron activity controls spatial learning and memory retrieval. PLoS One. 2012; 7:e40555. [PubMed: 22792368]

Autti-Rämö I, Granström ML. The psychomotor development during the first year of life of infants exposed to intrauterine alcohol of various duration. Fetal alcohol exposure and development. Neuropediatrics. 1991; 22:59–64. [PubMed: 1713311]

Ben-Ari Y. The GABA excitatory/inhibitory developmental sequence: a personal journey. Neuroscience. 2014; 279:187–219. [PubMed: 25168736]

Ben-Ari Y, Khalilov I, Kahle KT, Cherubini E. The GABA excitatory/inhibitory shift in brain maturation and neurological disorders. Neuroscientist. 2012; 18:467–486. [PubMed: 22547529]

Bering R, Draguhn A, Diemer NH, Johansen FF. Ischemia changes the coexpression of somatostatin and neuropeptide Y in hippocampal interneurons. Exp Brain Res. 1997; 115:423–429. [PubMed: 9262197]

Berman RF, Hannigan JH. Effects of prenatal alcohol exposure on the hippocampus: spatial behavior, electrophysiology, and neuroanatomy. Hippocampus. 2000; 10:94–110. [PubMed: 10706221]

Bird CW, Barto D, Magcalas CM, Rodriguez CI, Donaldson T, Davies S, Savage DD, Hamilton DA. Ifenprodil infusion in agranular insular cortex alters social behavior and vocalizations in rats exposed to moderate levels of ethanol during prenatal development. Behav Brain Res. 2017; 320:1–11. [PubMed: 27888019]

Camargo Moreno M, Mooney SM, Middleton FA. Heterogeneity of p53 dependent genomic responses following ethanol exposure in a developmental mouse model of fetal alcohol spectrum disorder. PLoS One. 2017; 12:e0180873. [PubMed: 28723918]

Cellot G, Cherubini E. Functional role of ambient GABA in refining neuronal circuits early in postnatal development. Front Neural Circuits. 2013; 7:136. [PubMed: 23964205]

Chasnoff IJ, Wells AM, Telford E, Schmidt C, Messer G. Neurodevelopmental functioning in children with FAS, pFAS, and ARND. J Dev Behav Pediatr. 2010; 31:192–201. [PubMed: 20375733]

Chi P, Aras R, Martin K, Favero C. Using Swiss Webster mice to model Fetal Alcohol Spectrum Disorders (FASD): An analysis of multilevel time-to-event data through mixed-effects Cox proportional hazards models. Behav Brain Res. 2016; 305:1–7. [PubMed: 26765502]

Cobb SR, Buhl EH, Halasy K, Paulsen O, Somogyi P. Synchronization of neuronal activity in hippocampus by individual GABAergic interneurons. Nature. 1995; 378:75–78. [PubMed: 7477292]

Cohen, J. Statistical Power Analysis for the Behavioral Sciences. New York, NY: Routledge Academic; 1988.

Cumming, G. Understanding the new statistics: effect sizes, confidence intervals, and meta-analysis. New York: Routledge, Taylor & Francis Group; 2012.

D'Amelio M, Cavallucci V, Cecconi F. Neuronal caspase-3 signaling: not only cell death. Cell Death Differ. 2010; 17:1104–1114. [PubMed: 19960023]

Elmore S. Apoptosis: a review of programmed cell death. Toxicol Pathol. 2007; 35:495–516. [PubMed: 17562483]

Erturk A, Wang Y, Sheng M. Local pruning of dendrites and spines by caspase-3-dependent and proteasome-limited mechanisms. J Neurosci. 2014; 34:1672–1688. [PubMed: 24478350]

Ethen MK, Ramadhani TA, Scheuerle AE, Canfield MA, Wyszynski DF, Druschel CM, Romitti PA, National Birth Defects Prevention S. Alcohol consumption by women before and during pregnancy. Matern Child Health J. 2009; 13:274–285. [PubMed: 18317893]

Freedman R, Wetmore C, Stromberg I, Leonard S, Olson L. Alpha-bungarotoxin binding to hippocampal interneurons: immunocytochemical characterization and effects on growth factor expression. J Neurosci. 1993; 13:1965–1975. [PubMed: 8478687]

Galindo R, Valenzuela CF. Immature hippocampal neuronal networks do not develop tolerance to the excitatory actions of ethanol. Alcohol. 2006; 40:111–118. [PubMed: 17307647]

Galindo R, Zamudio PA, Valenzuela CF. Alcohol is a potent stimulant of immature neuronal networks: implications for fetal alcohol spectrum disorder. J Neurochem. 2005; 94:1500–1511. [PubMed: 16000153]

Gulyaeva NV, Kudryashov IE, Kudryashova IV. Caspase activity is essential for long-term potentiation. J Neurosci Res. 2003; 73:853–864. [PubMed: 12949912]

Gundersen HJ, Jensen EB, Kieu K, Nielsen J. The efficiency of systematic sampling in stereology–reconsidered. J Microsc. 1999; 193:199–211. [PubMed: 10348656]

Hamilton DA, Kodituwakku P, Sutherland RJ, Savage DD. Children with Fetal Alcohol Syndrome are impaired at place learning but not cued-navigation in a virtual Morris water task. Behav Brain Res. 2003; 143:85–94. [PubMed: 12842299]

Hamilton GF, Murawski NJ, St Cyr SA, Jablonski SA, Schiffino FL, Stanton ME, Klintsova AY. Neonatal alcohol exposure disrupts hippocampal neurogenesis and contextual fear conditioning in adult rats. Brain Res. 2011; 1412:88–101. [PubMed: 21816390]

Hedges, LV., Olkin, I. Statistical methods for meta-analysis. Orlando: Academic Press; 1985.

Hellemans KG, Verma P, Yoon E, Yu WK, Young AH, Weinberg J. Prenatal alcohol exposure and chronic mild stress differentially alter depressive- and anxiety-like behaviors in male and female offspring. Alcohol Clin Exp Res. 2010; 34:633–645. [PubMed: 20102562]

Hochreiter-Hufford A, Ravichandran KS. Clearing the dead: apoptotic cell sensing, recognition, engulfment, and digestion. Cold Spring Harb Perspect Biol. 2013; 5:a008748. [PubMed: 23284042]

Huesmann GR, Clayton DF. Dynamic role of postsynaptic caspase-3 and BIRC4 in zebra finch song-response habituation. Neuron. 2006; 52:1061–1072. [PubMed: 17178408]

Ikonomidou C, Bittigau P, Ishimaru MJ, Wozniak DF, Koch C, Genz K, Price MT, Stefovska V, Horster F, Tenkova T, et al. Ethanol-induced apoptotic neurodegeneration and fetal alcohol syndrome. Science. 2000; 287:1056–1060. [PubMed: 10669420]

Johansen FF. Interneurons in rat hippocampus after cerebral ischemia. Morphometric, functional, and therapeutic investigations. Acta Neurol Scand Suppl. 1993; 150:1–32. [PubMed: 7907456]

Kajimoto K, Allan A, Cunningham LA. Fate analysis of adult hippocampal progenitors in a murine model of fetal alcohol spectrum disorder (FASD). PLoS One. 2013; 8:e73788. [PubMed: 24040071]

Kajimoto K, Valenzuela CF, Allan AM, Ge S, Gu Y, Cunningham LA. Prenatal alcohol exposure alters synaptic activity of adult hippocampal dentate granule cells under conditions of enriched environment. Hippocampus. 2016; 26:1078–1087. [PubMed: 27009742]

Klintsova AY, Helfer JL, Calizo LH, Dong WK, Goodlett CR, Greenough WT. Persistent impairment of hippocampal neurogenesis in young adult rats following early postnatal alcohol exposure. Alcohol Clin Exp Res. 2007; 31:2073–2082. [PubMed: 17949464]

Kodituwakku PW. Defining the behavioral phenotype in children with fetal alcohol spectrum disorders: a review. Neurosci Biobehav Rev. 2007; 31:192–201. [PubMed: 16930704]

Kullmann DM. Interneuron networks in the hippocampus. Curr Opin Neurobiol. 2011; 21:709–716. [PubMed: 21636266]

Lakens D. Calculating and reporting effect sizes to facilitate cumulative science: a practical primer for t-tests and ANOVAs. Front Psychol. 2013; 4:863. [PubMed: 24324449]

Le Magueresse C, Monyer H. GABAergic interneurons shape the functional maturation of the cortex. Neuron. 2013; 77:388–405. [PubMed: 23395369]

Lowenstein DH, Thomas MJ, Smith DH, McIntosh TK. Selective vulnerability of dentate hilar neurons following traumatic brain injury: a potential mechanistic link between head trauma and disorders of the hippocampus. J Neurosci. 1992; 12:4846–4853. [PubMed: 1464770]

Lubke J, Frotscher M, Spruston N. Specialized electrophysiological properties of anatomically identified neurons in the hilar region of the rat fascia dentata. J Neurophysiol. 1998; 79:1518–1534. [PubMed: 9497429]

Maccaferri G, Lacaille JC. Interneuron Diversity series: Hippocampal interneuron classifications–making things as simple as possible, not simpler. Trends Neurosci. 2003; 26:564–571. [PubMed: 14522150]

Mattson SN, Riley EP. Implicit and explicit memory functioning in children with heavy prenatal alcohol exposure. J Int Neuropsychol Soc. 1999; 5:462–471. [PubMed: 10439591]

Mattson SN, Riley EP, Delis DC, Stern C, Jones KL. Verbal learning and memory in children with fetal alcohol syndrome. Alcohol Clin Exp Res. 1996; 20:810–816. [PubMed: 8865953]

Mattson SN, Roesch SC, Glass L, Deweese BN, Coles CD, Kable JA, May PA, Kalberg WO, Sowell ER, Adnams CM, et al. Further development of a neurobehavioral profile of fetal alcohol spectrum disorders. Alcohol Clin Exp Res. 2013; 37:517–528. [PubMed: 22974253]

May PA, Baete A, Russo J, Elliott AJ, Blankenship J, Kalberg WO, Buckley D, Brooks M, Hasken J, Abdul-Rahman O, et al. Prevalence and characteristics of fetal alcohol spectrum disorders. Pediatrics. 2014; 134:855–866. [PubMed: 25349310]

Miguez HA, Magri R, Suarez M. Consumo de tabaco y bebidas alcohólicas durante el embarazo. Acta Psiquiátrica y Psicológica de América Latina. 2009; 55:76–83.

Miki T, Harris SJ, Wilce P, Takeuchi Y, Bedi KS. Neurons in the hilus region of the rat hippocampus are depleted in number by exposure to alcohol during early postnatal life. Hippocampus. 2000; 10:284–295. [PubMed: 10902898]

Miller MW. Effect of prenatal exposure to ethanol on glutamate and GABA immunoreactivity in macaque somatosensory and motor cortices: critical timing of exposure. Neuroscience. 2006; 138:97–107. [PubMed: 16427209]

Moore DB, Quintero MA, Ruygrok AC, Walker DW, Heaton MB. Prenatal ethanol exposure reduces parvalbumin-immunoreactive GABAergic neuronal number in the adult rat cingulate cortex. Neurosci Lett. 1998; 249:25–28. [PubMed: 9672380]

Morton RA, Diaz MR, Topper LA, Valenzuela CF. Construction of vapor chambers used to expose mice to alcohol during the equivalent of all three trimesters of human development. J Vis Exp. 2014

Muller C, Remy S. Dendritic inhibition mediated by O-LM and bistratified interneurons in the hippocampus. Front Synaptic Neurosci. 2014; 6:23. [PubMed: 25324774]

Myers CE, Scharfman HE. A role for hilar cells in pattern separation in the dentate gyrus: a computational approach. Hippocampus. 2009; 19:321–337. [PubMed: 18958849]

Nirgudkar P, Taylor DH, Yanagawa Y, Valenzuela CF. Ethanol exposure during development reduces GABAergic/glycinergic neuron numbers and lobule volumes in the mouse cerebellar vermis. Neurosci Lett. 2016; 632:86–91. [PubMed: 27565053]

Noor S, Sanchez JJ, Vanderwall AG, Sun MS, Maxwell JR, Davies S, Jantzie LL, Petersen TR, Savage DD, Milligan ED. Prenatal alcohol exposure potentiates chronic neuropathic pain, spinal glial and immune cell activation and alters sciatic nerve and DRG cytokine levels. Brain Behav Immun. 2017; 61:80–95. [PubMed: 28011263]

Ogievetsky E, Lotfullina N, Minlebaeva A, Khazipov R. Ethanol-Induced Apoptosis of Interneurons in the Neonatal GAD67-GFP Mouse Hippocampus. BioNanoScience. 2017; 7:151–154.

Ognjanovski N, Schaeffer S, Wu J, Mofakham S, Maruyama D, Zochowski M, Aton SJ. Parvalbumin-expressing interneurons coordinate hippocampal network dynamics required for memory consolidation. Nat Commun. 2017; 8:15039. [PubMed: 28382952]

Olbrich HG, Braak H. Ratio of pyramidal cells versus non-pyramidal cells in sector CA1 of the human Ammon's horn. Anat Embryol (Berl). 1985; 173:105–110. [PubMed: 4073527]

Olney JW, Tenkova T, Dikranian K, Muglia LJ, Jermakowicz WJ, D'Sa C, Roth KA. Ethanol-induced caspase-3 activation in the in vivo developing mouse brain. Neurobiol Dis. 2002; 9:205–219. [PubMed: 11895372]

Paxinos, G., Franklin, KBJ. Paxinos and Franklin's The Mouse Brain in Stereotaxic Coordinates. Fourth. Elsevier; 2013.

Preibisch S, Saalfeld S, Tomancak P. Globally optimal stitching of tiled 3D microscopic image acquisitions. Bioinformatics. 2009; 25:1463–1465. [PubMed: 19346324]

Ribak CE, Shapiro LA. Ultrastructure and synaptic connectivity of cell types in the adult rat dentate gyrus. Prog Brain Res. 2007; 163:155–166. [PubMed: 17765717]

Riley EP, Infante MA, Warren KR. Fetal alcohol spectrum disorders: an overview. Neuropsychol Rev. 2011; 21:73–80. [PubMed: 21499711]

Rodriguez CI, Davies S, Calhoun V, Savage DD, Hamilton DA. Moderate Prenatal Alcohol Exposure Alters Functional Connectivity in the Adult Rat Brain. Alcohol Clin Exp Res. 2016a; 40:2134–2146. [PubMed: 27570053]

Rodriguez CI, Magcalas CM, Barto D, Fink BC, Rice JP, Bird CW, Davies S, Pentkowski NS, Savage DD, Hamilton DA. Effects of sex and housing on social, spatial, and motor behavior in adult rats exposed to moderate levels of alcohol during prenatal development. Behavioural Brain Research. 2016b In Press.

Sadrian B, Lopez-Guzman M, Wilson DA, Saito M. Distinct neurobehavioral dysfunction based on the timing of developmental binge-like alcohol exposure. Neuroscience. 2014; 280:204–219. [PubMed: 25241068]

Savanthrapadian S, Meyer T, Elgueta C, Booker SA, Vida I, Bartos M. Synaptic properties of SOM- and CCK-expressing cells in dentate gyrus interneuron networks. J Neurosci. 2014; 34:8197–8209. [PubMed: 24920624]

Schiavone S, Neri M, Trabace L, Turillazzi E. The NADPH oxidase NOX2 mediates loss of parvalbumin interneurons in traumatic brain injury: human autoptic immunohistochemical evidence. Sci Rep. 2017; 7:8752. [PubMed: 28821783]

Schneider CA, Rasband WS, Eliceiri KW. NIH Image to ImageJ: 25 years of image analysis. Nat Methods. 2012; 9:671–675. [PubMed: 22930834]

Semple BD, Blomgren K, Gimlin K, Ferriero DM, Noble-Haeusslein LJ. Brain development in rodents and humans: Identifying benchmarks of maturation and vulnerability to injury across species. Prog Neurobiol. 2013; 106–107:1–16.

Shetty AK, Hattiangady B, Rao MS. Vulnerability of hippocampal GABA-ergic interneurons to kainate-induced excitotoxic injury during old age. J Cell Mol Med. 2009; 13:2408–2423. [PubMed: 20141618]

Shetty AK, Turner DA. Glutamic acid decarboxylase-67-positive hippocampal interneurons undergo a permanent reduction in number following kainic acid-induced degeneration of ca3 pyramidal neurons. Exp Neurol. 2001; 169:276–297. [PubMed: 11358442]

Simmons RW, Thomas JD, Levy SS, Riley EP. Motor response programming and movement time in children with heavy prenatal alcohol exposure. Alcohol. 2010; 44:371–378. [PubMed: 20598488]

Smiley JF, Saito M, Bleiwas C, Masiello K, Ardekani B, Guilfoyle DN, Gerum S, Wilson DA, Vadasz C. Selective reduction of cerebral cortex GABA neurons in a late gestation model of fetal alcohol spectrum disorder. Alcohol. 2015; 49:571–580. [PubMed: 26252988]

Staples MC, Kim A, Mandyam CD. Dendritic remodeling of hippocampal neurons is associated with altered NMDA receptor expression in alcohol dependent rats. Mol Cell Neurosci. 2015; 65:153–162. [PubMed: 25769285]

Stepanichev MY, Kudryashova IV, Yakovlev AA, Onufriev MV, Khaspekov LG, Lyzhin AA, Lazareva NA, Gulyaeva NV. Central administration of a caspase inhibitor impairs shuttle-box performance in rats. Neuroscience. 2005; 136:579–591. [PubMed: 16198488]

Thanh NX, Jonsson E, Salmon A, Sebastianski M. Incidence and prevalence of fetal alcohol spectrum disorder by sex and age group in Alberta, Canada. J Popul Ther Clin Pharmacol. 2014; 21:e395–404. [PubMed: 25381628]

Topper LA, Baculis BC, Valenzuela CF. Exposure of neonatal rats to alcohol has differential effects on neuroinflammation and neuronal survival in the cerebellum and hippocampus. J Neuroinflammation. 2015; 12:160. [PubMed: 26337952]

Tunc-Ozcan E, Wert SL, Lim PH, Ferreira A, Redei EE. Hippocampus-dependent memory and allele-specific gene expression in adult offspring of alcohol-consuming dams after neonatal treatment with thyroxin or metformin. Mol Psychiatry. 2017

Uecker A, Nadel L. Spatial locations gone awry: object and spatial memory deficits in children with fetal alcohol syndrome. Neuropsychologia. 1996; 34:209–223. [PubMed: 8868278]

Uecker A, Nadel L. Spatial but not object memory impairments in children with fetal alcohol syndrome. Am J Ment Retard. 1998; 103:12–18. [PubMed: 9678226]

Valeeva G, Valiullina F, Khazipov R. Excitatory actions of GABA in the intact neonatal rodent hippocampus in vitro. Front Cell Neurosci. 2013; 7:20. [PubMed: 23467988]

Varaschin RK, Akers KG, Rosenberg MJ, Hamilton DA, Savage DD. Effects of the cognition-enhancing agent ABT-239 on fetal ethanol-induced deficits in dentate gyrus synaptic plasticity. J Pharmacol Exp Ther. 2010; 334:191–198. [PubMed: 20308329]

Varlinskaya EI, Mooney SM. Acute exposure to ethanol on gestational day 15 affects social motivation of female offspring. Behav Brain Res. 2014; 261:106–109. [PubMed: 24355753]

Viollet C, Simon A, Tolle V, Labarthe A, Grouselle D, Loe-Mie Y, Simonneau M, Martel G, Epelbaum J. Somatostatin-IRES-Cre Mice: Between Knockout and Wild-Type? Front Endocrinol (Lausanne). 2017; 8:131. [PubMed: 28674519]

Wang Y, Kakizaki T, Sakagami H, Saito K, Ebihara S, Kato M, Hirabayashi M, Saito Y, Furuya N, Yanagawa Y. Fluorescent labeling of both GABAergic and glycinergic neurons in vesicular GABA transporter (VGAT)-venus transgenic mouse. Neuroscience. 2009; 164:1031–1043. [PubMed: 19766173]

West JR. Fetal alcohol-induced brain damage and the problem of determining temporal vulnerability: a review. Alcohol Drug Res. 1987; 7:423–441. [PubMed: 3304313]

Wilson DA, Peterson J, Basavaraj BS, Saito M. Local and regional network function in behaviorally relevant cortical circuits of adult mice following postnatal alcohol exposure. Alcohol Clin Exp Res. 2011; 35:1974–1984. [PubMed: 21649667]

Wu JY, Henins KA, Gressens P, Gozes I, Fridkin M, Brenneman DE, Hill JM. Neurobehavioral development of neonatal mice following blockade of VIP during the early embryonic period. Peptides. 1997; 18:1131–1137. [PubMed: 9396053]

HIGHLIGHTS

- We studied the effects of third trimester ethanol exposure on interneurons
- Venus-VGAT mice were exposed to ethanol in vapor chambers (postnatal days 2-9)
- At postnatal day 7 ethanol activates caspase-3 in hippocampal interneurons
- At postnatal day 90 ethanol reduced hippocampal interneurons numbers in males
- Significant effects in males at P90 were seen in the hilus, CA1, and CA3 subfields

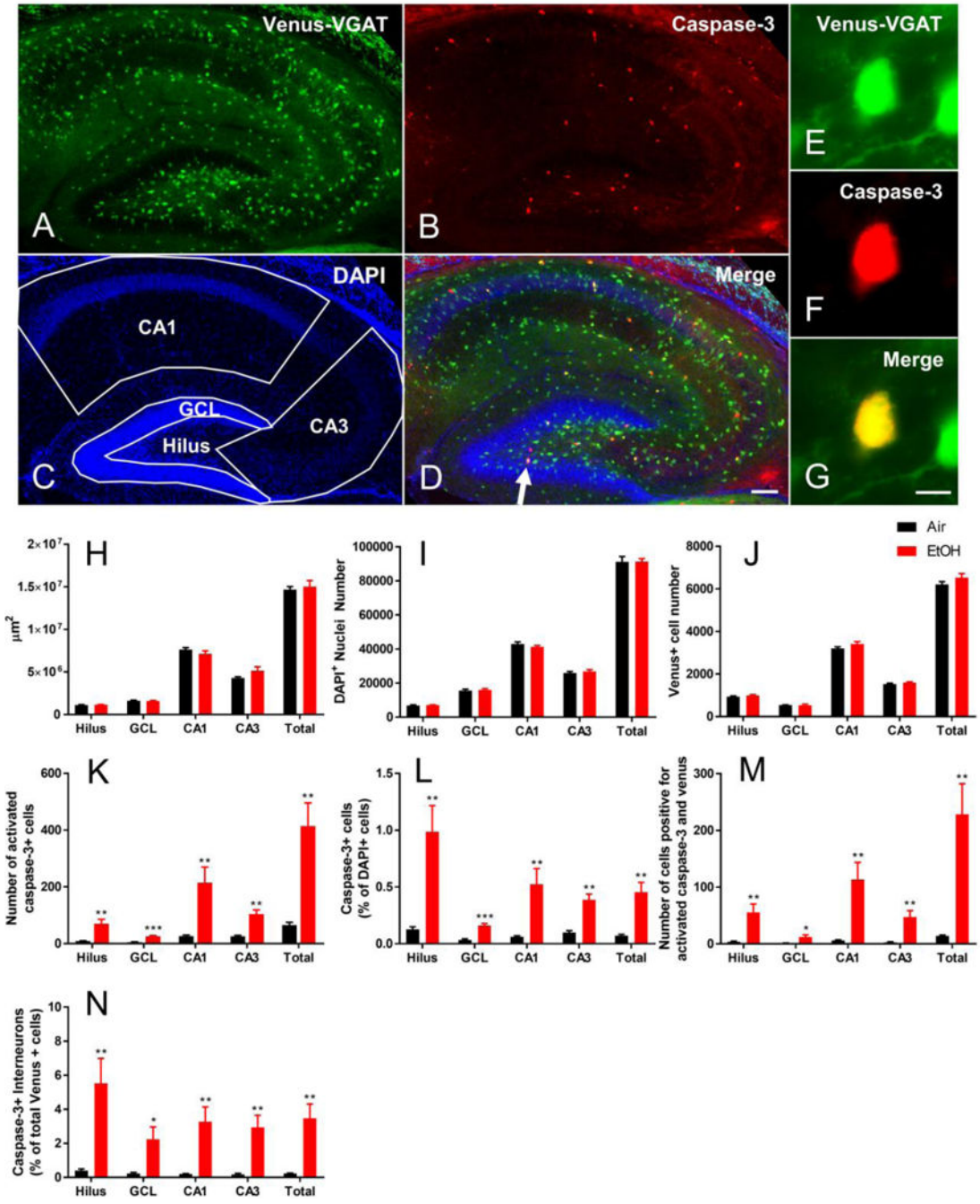

Figure 1.

Exposure to EtOH at P7 activates apoptotic pathways in interneurons of the mouse hippocampus. An example of activated caspase-3 immunohistochemistry from an EtOH-exposed Venus-VGAT^{+} mouse is presented in A-D (10× objective; scale bar = 100μm), with a high magnification image of an activated-caspase-3 expressing Venus^{+} interneuron shown in E-G (40× objective, scale bar = 10 μm). (A) Venus fluorescence driven by VGAT promoter in hippocampal interneurons. (B) Activated caspase-3 immunochemistry. (C) DAPI staining of nuclei within the hippocampus, along with contours used for counting

interneurons, cleaved caspase-3 positive cells, and cleaved caspase-3 positive interneurons. (D) Merged image used for colocalization. The arrow points to the cell used for high magnification images shown in E-G. (E) Venus fluorescence at high magnification. (F) Cleaved caspase-3 immunofluorescence at high magnification. (G) Merged Venus and cleaved caspase-3 demonstrating colocalization at high magnification. (H) The total area in μm^2 of each hippocampal region analyzed for both vapor chamber exposure conditions is presented. (I) The total number of $DAPI^+$ nuclei in each hippocampal region. (J) The number of Venus positive interneurons in the hippocampus. (K) Cleaved caspase-3 positive cells in each hippocampal region. (L) Cleaved caspase-3 positive cells as a percentage of total DAPI nuclei in the hippocampus. (M) Number of activated-caspase-3 expressing $Venus^+$ interneurons in the hippocampus. (N) Percent of Venus+ cells that were positive for activated caspase-3. Data are presented as mean + SEM. Black bars represent air-exposed mice, red bars represent EtOH-exposed mice. Asterisk(*) denotes a significant between-subjects effect of vapor chamber exposure condition within region from repeated measures ANOVA at $p < 0.05$, ** $p < 0.01$, *** $p < 0.001$. $n = 5$ mice per vapor chamber exposure condition.

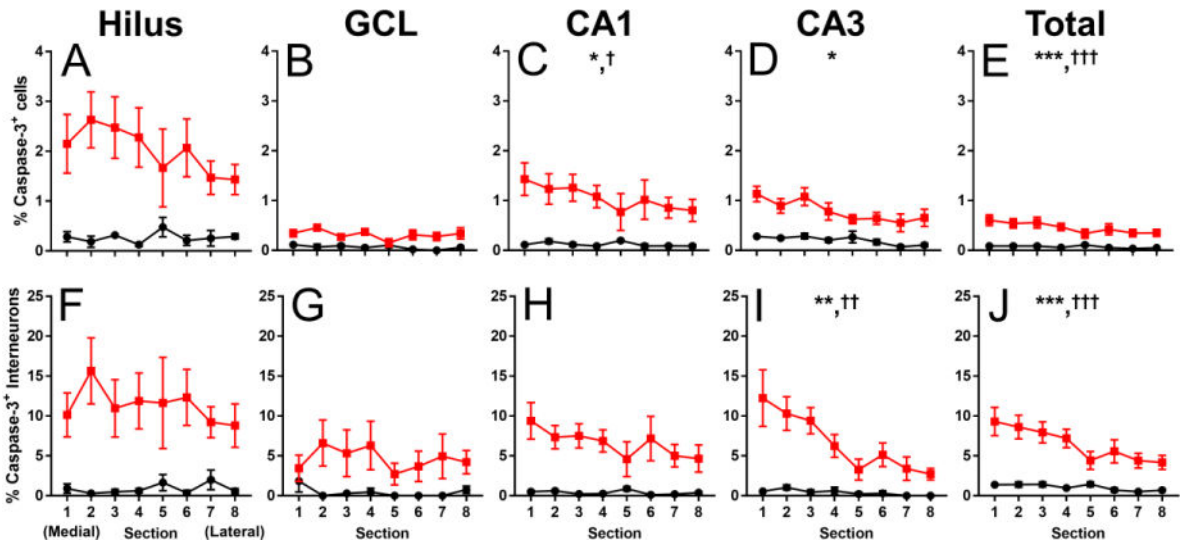

Figure 2.

Medial to lateral gradient of activated caspase-3 positive cells and interneurons in the hippocampus at P7. (A-E) The percent of activated caspase-3 positive cells as a percentage of total DAPI nuclei in every medial (section 1) to lateral (section 8) section in the hilus (A), GCL (B), CA1 (C), CA3 (D), and combined hippocampal regions (E). (F-J) The percent of activated caspase-3 positive interneurons as a function of total Venus-$^{+}$ cells in every medial to lateral section in the hilus (F), GCL (G), CA1 (H), CA3 (I), and combined hippocampal regions (J). Black circles represent air-exposed mice, red squares represent EtOH-exposed mice. Asterisk(*) denotes a significant within-subjects effect of medial to lateral tissue section on the percentage of either activated caspase-3 positive cells or activated caspase-3 positive interneurons at $p < 0.05$, ** $p < 0.01$, *** $p < 0.001$. Dagger(†) denotes a significant interaction of medial to lateral tissue section and vapor chamber exposure condition on the percentage of activated caspase-3 positive cells at $p < 0.05$, †† $p < 0.01$, ††† $p < 0.001$. n = 5 mice per vapor chamber exposure condition.

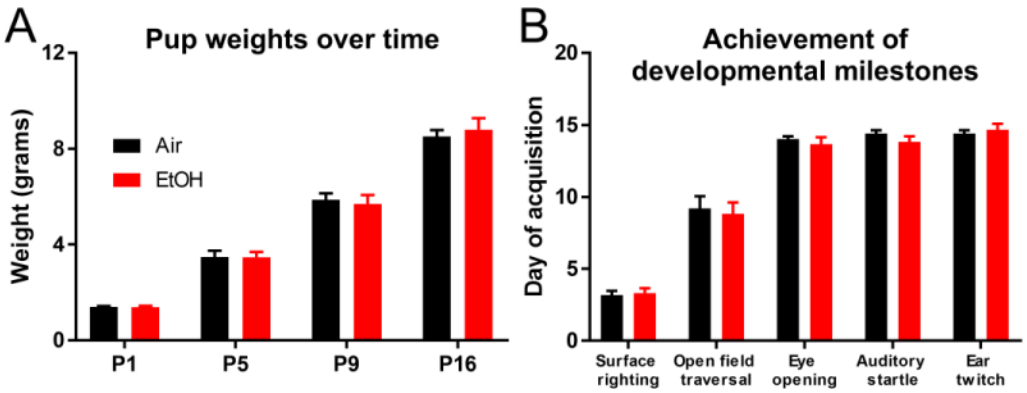

Figure 3.

Similar development of Venus-VGAT^{+} pups between vapor chamber-exposure conditions. (A) Pups weights (mean + SEM) from both vapor chamber exposure condition before (P1) during (P5 and P9) and after (P16) vapor chamber exposure to monitor pup growth over time. P1: air n = 12 litters, EtOH n = 10 litters; P5: air n = 6 litters, EtOH n = 6 litters; P9: air n = 11 litters, EtOH n = 9 litters; P16: air n = 10 litters, EtOH = 8 litters. (B) The day (mean + SEM) pups acquired the following developmental milestones: surface righting reflex, ability to cross an open field, eye opening, display of an auditory startle reflex, and ear twitch in response to tactile stimulation. Black bars represent air-exposed mice, red bars represent EtOH-exposed mice. n = 6 litters per vapor chamber exposure condition.

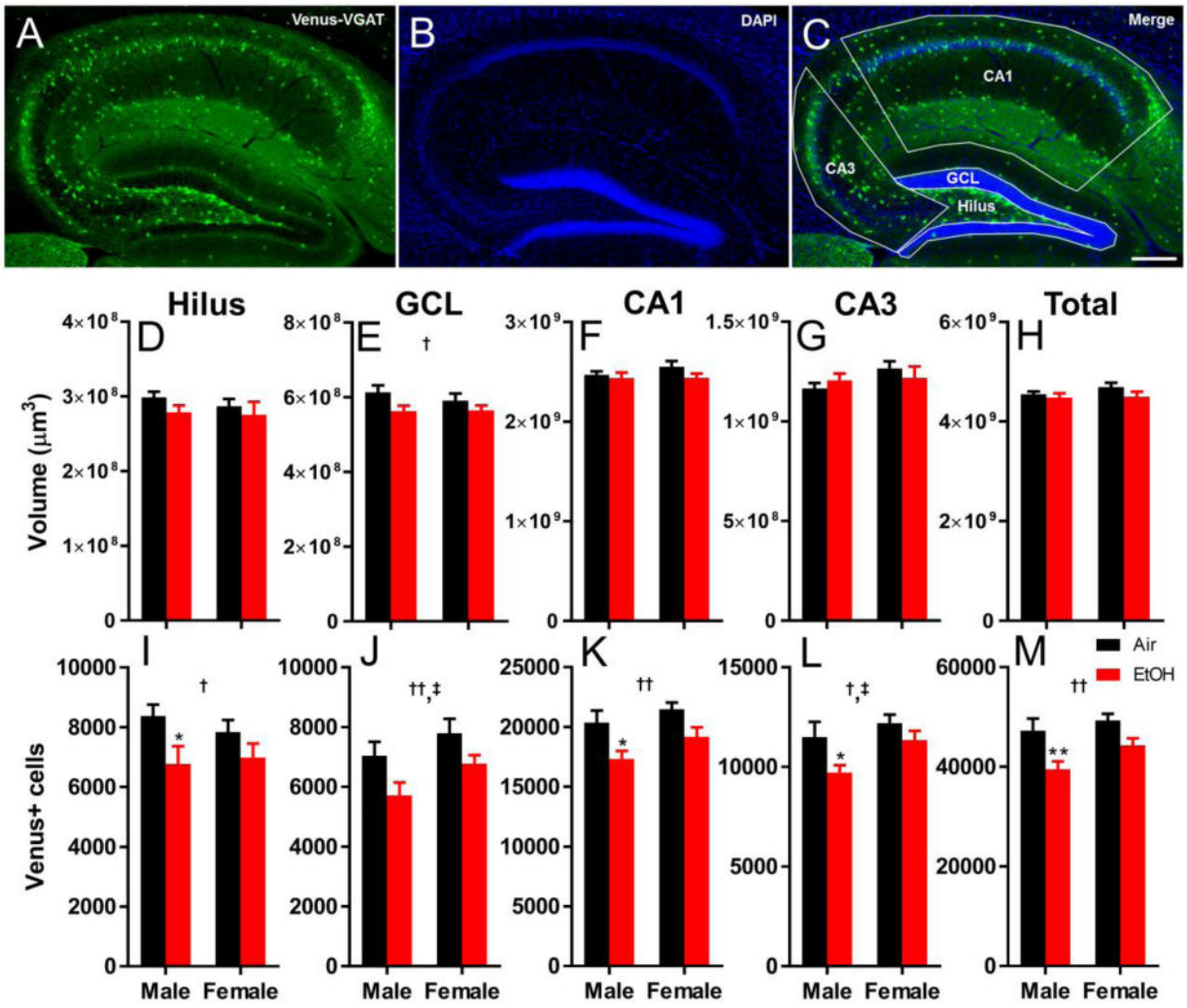

Figure 4.

Third trimester-equivalent EtOH exposure causes a long-term reduction in the population of hippocampal interneurons measured at P90. An example of a DAPI counterstained hippocampus from an air-exposed male Venus-VGAT^{+} mouse brain is presented in A-C. Scale bar = 200 μm. (A) Venus+ interneurons. (B) DAPI stained nuclei. (C) Merged image with example contours used for unbiased stereological measurements. (D-H) Volumes in μm^3 are presented for the hilus (D), granule cell layer (GCL) (E), CA1 (F), CA3 (G), and combined regions (H) of the hippocampus from both sexes and vapor chamber exposure conditions. (I-M) Stereological estimation of total Venus-VGAT interneuron populations from both exposure conditions in the hilus (I), GCL (J), CA1 (K), CA3 (L), and combined regions (M) of the hippocampus from both sexes and exposure conditions. Graphs are presented as mean + SEM. Black bars represent air-exposed mice, red bars represent EtOH-exposed mice. Asterisk(*) denotes a significant effect from Sidak post hoc analysis of vapor chamber exposure condition within sex and region at $p < 0.05$, ** $p < 0.01$. Dagger(†) denotes a significant effect of vapor chamber exposure condition within region at † $p < 0.05$,

†† $p < 0.01$. Double dagger (‡) denotes a significant effect of sex on interneuron count within region at $p < 0.05$. n = 8 mice per sex and vapor chamber exposure condition.

Table 1

Maternal care measures. Immediately following vapor chamber exposure on P2 and P5, maternal care was assessed in mouse dams from both vapor chamber exposure conditions. Data presented are mean(SEM) latency measured in seconds. n = 6 litters per vapor chamber exposure condition.

Parameter measured	Air	EtOH
Dam latency to displaced pups P2	**9.00**(2.78)	**7.80**(1.87)
Dam latency to displaced pups P5	**8.16**(1.33)	**7.83**(1.47)
Dam latency to retrieve displaced pups P2	**43.5**(18.41)	**41.17**(14.21)
Dam latency to retrieve displaced pups P5	**23.17**(7.02)	**30.50**(8.94)
Dam latency to rebuild nest P2	**119.7**(23.28)	**154.2**(13.06)
Dam latency to rebuild nest P5	**156.3**(27.71)	**116.7**(17.90)